

Local Hole revisited: evidence for bulk motions and self-consistent outflow

T. Shanks¹,^{*} L.M. Hogarth², N. Metcalfe¹, J. Whitbourn¹.

¹*Department of Physics, Durham University, South Road, Durham, DH1 3LE, England*

²*Department of Physics and Astronomy, University College London, Gower Street, London WC1E 6BT, England*

Accepted 2019... . Received 2019.....; in original form 2019 May 5

ABSTRACT

We revisit our mapping of the ‘Local Hole’, a large underdensity in the local galaxy redshift distribution that extends out to redshift, $z \approx 0.05$ and a potential source of outflows that may perturb the global expansion rate and thus help mitigate the present ‘ H_0 tension’. First, we compare local peculiar velocities measured via the galaxy average redshift-magnitude Hubble diagram, $\bar{z}(m)$, with a simple dynamical outflow model based on the average underdensity in the Local Hole. We find that this outflow model is in good agreement with our peculiar velocity measurements from $\bar{z}(m)$ and not significantly inconsistent with SNIa peculiar velocity measurements from at least the largest previous survey. This outflow could cause an $\approx 2-3\%$ increase in the local value of Hubble’s constant. Second, considering anisotropic motions, we find that the addition of the outflow model may improve the $\bar{z}(m)$ fit of a bulk flow where galaxies are otherwise at rest in the Local Group frame. We conclude that the Local Hole plus neighbouring overdensities such as the Shapley Supercluster may cause outflow and bulk motions out to $\approx 150h^{-1}\text{Mpc}$ that are cosmologically significant and that need to be taken into account in estimating Hubble’s constant.

Key words: cosmology – distance scale – Hubble’s Constant

1 INTRODUCTION

There have been many studies of large scale structure of the Local Universe. While the Local Group and the Local Supercluster on ≈ 1 and $\approx 10h^{-1}\text{Mpc}$ scales are now well established, there is still controversy over the possible existence of larger scale structures (e.g. Watkins et al. (2009); Davis et al. (2011); Nusser et al. (2011); Macaulay et al. (2011, 2012); Turnbull et al. (2012); Davis & Scrimgeour (2014); Watkins & Feldman (2015); Nusser (2014, 2016); Scrimgeour et al. (2016); Feix et al. (2017)). Evidence for bulk motions originally suggested the presence of a ‘Great’ or ‘Giant Attractor’ either at $\approx 40h^{-1}\text{Mpc}$ or $\approx 150h^{-1}\text{Mpc}$ scales corresponding respectively to the Hydra-Centaurus (see e.g. Lynden-Bell et al. (1988)) or Shapley superclusters (see e.g. Mathewson et al. (1992); Lauer & Postman (1992, 1994); Tonry et al. (2000)) and references therein. These studies generally use standard candles to provide galaxy distances from which their ‘peculiar motions’ can be derived from their redshifts and sophisticated modelling procedures were developed to compare the peculiar velocities and density fields to derive cosmological parameters (see e.g. Dekel et al. (1999); Carrick et al. (2015); Jasche & Lavaux (2019)). In the later references the ear-

lier claims for bulk motions of significant amplitude become more muted as the CMB evidence mounted for models with $\Omega_m \approx 0.3$ rather than $\Omega_m = 1$ (e.g. Spergel et al. (2003); Planck Collaboration et al. (2018)). In addition, a ‘Local Hole’ has also been claimed particularly in the Southern Galactic Cap (SGC) out to $\approx 150h^{-1}\text{Mpc}$ (see e.g. Shanks et al. (1984); Frith et al. (2003); Busswell et al. (2004); Keenan et al. (2012); Whitbourn & Shanks (2014, 2016)). These latter studies are mainly based on observations of galaxy clustering via galaxy counts in redshift surveys. Other authors have also claimed the existence of smaller-scale local voids e.g. Tully et al. (2008, 2016); Rizzi et al. (2017); Pustilnik et al. (2019).

There are several other arguments supporting the idea that the Universe may be more inhomogeneous than expected. In terms of the Local Hole there is striking agreement between the galaxy number redshift distribution, $n(z)$, of Whitbourn & Shanks (2014) (WS14) and the galaxy cluster $n(z)$ from the REFLEX II/CLASSIX X-ray samples of Böhringer et al. (2015, 2019) across the sky (see also Section 4).

More theoretically, the SNIa and BAO Hubble diagrams produce evidence for a cosmological constant which appears uncomfortably finely tuned and this has led several authors to look for an escape route by hypothesising a large local underdensity out to $z \approx 0.4$, usually modelled by

* E-mail: tom.shanks@durham.ac.uk (TS)

a Lemaitre-Tolman-Bondi (LTB) non-Copernican cosmology (e.g. Redlich et al. (2014)). Others (e.g. Luković et al. (2019)) have used the LTB approach with the more restricted aim of addressing the ‘ H_0 tension’ between Cosmic Microwave Background (Planck Collaboration et al. 2018) and local distance scale (e.g. Riess et al. (2018b,c) estimates of Hubble’s Constant, H_0).

Many of the claims of bulk motions and local underdensities are unlikely in the standard Λ CDM model. For example, Wu & Huterer (2017) suggest that the likely amplitude of velocity fluctuation in the local $\approx 150h^{-1}\text{Mpc}$ volume of WS14 is $\lesssim 5\%$ of what is needed to explain the current difference between global and local H_0 estimates. Indeed, Riess et al. (2018a) criticise the Local Hole velocity outflow model of Shanks et al. (2019) on the same grounds, that its $\approx 500\text{kms}^{-1}$ amplitude on $\approx 100h^{-1}\text{Mpc}$ scales is unlikely under Λ CDM at the 6σ level. Shanks et al. (2018) already argued that on their reading of the Wu & Huterer (2017) and Odderskov et al. (2017) papers, the significance under Λ CDM was lower, in the range $1.9\text{--}3.9\sigma$. Of course, whether it is more plausible to appeal to ‘new physics’ outside Λ CDM to explain the H_0 tension rather than the Local Hole can be debated. We also note that other authors emphasise that local underdensities compatible with Λ CDM at the $\approx 2\sigma$ level can at least partly explain the H_0 tension (e.g. Wojtak et al. 2014).

Here we return to consider the results of WS14 on the underdensity and dynamics of the Local Hole. Shanks et al. (2019) used a simple linear theory model to predict the outflow caused by this local underdensity and, assuming that it was centred on our position, found that it would make an $\approx 2\%$ reduction to the local distance scale estimate of Hubble’s Constant. Riess et al. (2018a); D’Arcy Kenworthy et al. (2019) criticised the assumption that the underdensity was isotropic around our position. Following Riess et al. (2018a), these authors also claimed that SNIa peculiar velocities from Scolnic et al. (2018) showed that the effect of any local underdensity was lower than suggested by Shanks et al. (2019). In what follows we shall address both these issues, the isotropy assumption in Section 2 and the SNIa results in Section 3.3. However, our main aim is to compare the outflow model of Shanks et al. (2019) based on the Local Hole underdensity estimates of WS14 with the independent peculiar velocity estimates of these authors and check for consistency (see Section 3.2).

The structure of the paper is therefore as follows. In Section 2 we first summarise the datasets and results used by WS14 and Whitbourn & Shanks (2016); we also review the evidence for the approximate isotropy of the ‘Local Hole’ around our position. Then, in Section 3, for the first time, we directly compare the peculiar velocities estimated by WS14 via the statistical Hubble diagram, $\bar{z}(m)$, of Soneira (1979) with the outflow velocity estimates from the dynamical model of Shanks et al. (2019). We further compare these with peculiar velocities estimated from the Pantheon SNIa survey of Scolnic et al. (2018) and the larger survey used by D’Arcy Kenworthy et al. (2019). We present our conclusions in Section 4. Throughout we shall assume a cosmology with $\Omega_\Lambda = 0.7$, $\Omega_m = 0.3$ and $H_0 = 100h\text{ km s}^{-1}\text{ Mpc}^{-1}$.

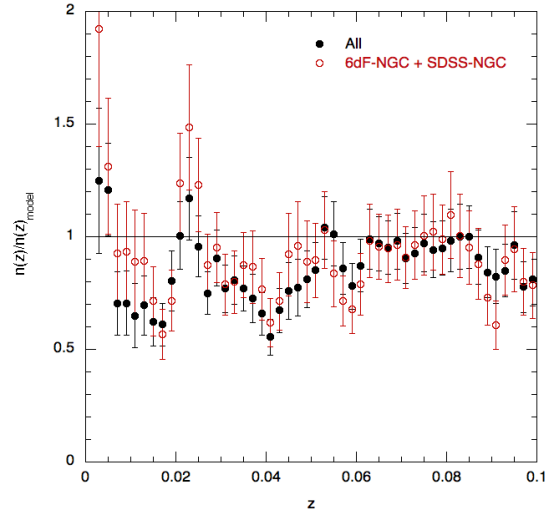


Figure 1. Density contrast-redshift relations for all three WS14 fields and for 6dF-NGC+SDSS-NGC, each combined by area weighting. These both show an underdensity out to $z \approx 0.05$ implying that the underdensity is not just restricted to the 6dF-SGC area and that our assumption of an approximately isotropic ‘Local Hole’ around our position is not unreasonable.

2 PREVIOUS DATASETS AND RESULTS

WS14 used 2MASS K band photometry to $K < 12.5$ to define the galaxy samples on which both their galaxy $n(z)$ distributions and peculiar velocity estimates were based. They worked in three sky regions covering $\approx 3000\text{deg}^2$ each for a total of 9161.7 deg^2 as given in their Table 2 and shown in their Fig. 1. They also used the galaxy redshift surveys 6dF-GRS for the two areas with Declination $\delta < 0^\circ$ and SDSS for the area with $\delta > 0^\circ$. The three areas are therefore termed 6dF-NGC, 6dF-SGC and SDSS-NGC. Roughly speaking, SDSS-NGC is centred on the North Galactic Pole, 6dF-SGC is centred on the South Galactic Pole and 6dF-NGC is in the direction of the CMB dipole and the Shapley Supercluster. WS14 first compared galaxy $n(z)$ distributions in these three areas with a homogeneous model based on an assumed galaxy luminosity function (LF). 2MASS+GAMA K -band galaxy counts were also used in consistency checks on the normalisation used in the model LF to estimate the over- and under-densities from the $n(z)$ at $K < 12.5$. Underdensities were detected in all three directions but most strongly in the 6dF-SGC direction. These results were checked by Whitbourn & Shanks (2016) who used maximum-likelihood methods to derive the density-redshift relations independently of the LF and found these $n(z)$ -based results to be robust.

The average galaxy redshift, \bar{z} , in $0.5\text{ mag } K$ bins was then plotted versus K magnitude in a Hubble diagram (see Fig. 13 of WS14). Soneira (1979) originally suggested using the statistic $\bar{z}(m)$ to test the linearity of the Hubble law in local galaxy redshift surveys complete to some magnitude limit, in our case $K < 12.5$. Here, the K band galaxy LF is implicitly assumed to be a standard candle out to $z \lesssim 0.1$. It is relatively easy to predict $\bar{z}(m)$ for the homogeneous case in the same way that galaxy number-magnitude, $n(m)$, count models can be calculated. Indeed, in the case of a Euclidean model, the prediction is simply that $\bar{z}(m) \propto 10^{0.2m}$. The

effects of cosmology, K-correction and evolution are easily included in the model. The LF normalisation $\phi^*(z)$ can also be used to eliminate the effects of large-scale structure. The residual between the observed $\bar{z}(K)$ Hubble diagram and the homogeneous model is then an estimate of the peculiar velocity.

WS14 found that two directions showed evidence of bulk motion ie galaxies at rest in the Local Group frame, while the surveyed galaxies in the third 6dF-SGC direction were more consistent with being at rest in the CMB frame. WS14 conjectured that the 6dF-SGC direction with its large underdensity might be additionally affected by outflows which, if included, might improve the fit of bulk motion in the Local Group frame. We return to this point in Section 3.2.

Finally, we shall also use the SNIa Pantheon survey of Scolnic et al. (2018). These include 1048 SNIa and are the data used by Riess et al. (2018b) to draw their Hubble diagram used to estimate H_0 . The same data plus additional unpublished Foundation+CSPDR3 SNIa surveys was used by D’Arcy Kenworthy et al. (2019) to search for any velocity outflow associated with the Local Hole. They concluded that the effect on H_0 was negligible. Here we use the 295 SNIa with $z < 0.15$ in the Pantheon sample of Scolnic et al. (2018) to compare with the $\bar{z}(m)$ peculiar velocities of WS14. We note that the statistical precision will be reduced by the loss of the Foundation+CSPDR3 surveys’ 102 SNIa with $0.023 < z < 0.15$. Also, both SNIa surveys have very non-isotropic sky coverage (see Fig. 3 of D’Arcy Kenworthy et al. (2019)). This leaves only 6 SNIa in 6dF-NGC, 29 in 6dF-SGC and 20 in SDSS-NGC in the required $0.02 < z < 0.05$ redshift range in the Pantheon survey. But we shall also compare these results to those from the full Pantheon+Foundation+CSPDR3 survey as reported by D’Arcy Kenworthy et al. (2019).

3 OBSERVED VS. PREDICTED OUTFLOWS

3.1 Predicted outflow model

Shanks et al. (2019) based their predicted ‘Local Hole’ outflow model on a simple linear theory gravitational growth model based on an assumed isotropic local galaxy underdensity as follows:

$$\frac{\Delta v}{v_H} = -\frac{1}{3} \frac{\delta \rho_g(< r)}{\bar{\rho}_g} \frac{\Omega_m^{0.6}}{b} \quad (1)$$

where Δv is the peculiar velocity at Hubble velocity, v_H , corresponding to comoving radius, r , and b is the galaxy bias. $\delta \rho_g(r)/\bar{\rho}_g$ is the density contrast given by

$$\frac{\delta \rho_g(< r)}{\bar{\rho}_g} = \frac{1}{V(r)} \sum_i \left(\frac{dn}{n} \right)_i 4\pi r_i^2 \delta r. \quad (2)$$

where $(\frac{dn}{n})_i$ are taken from averaging the data shown in Fig. 3 (a, b, c) of WS14. r_i are the corresponding comoving distances, δr is the comoving bin size and $V(r)$ is the spherical volume to radius, r . Clearly it is the 4π factor in eq. 2 that represents our assumption that the $(\frac{dn}{n})_i$ apply isotropically over the whole sky.

Since WS14 only showed the individual $n(z)$ ’s for their

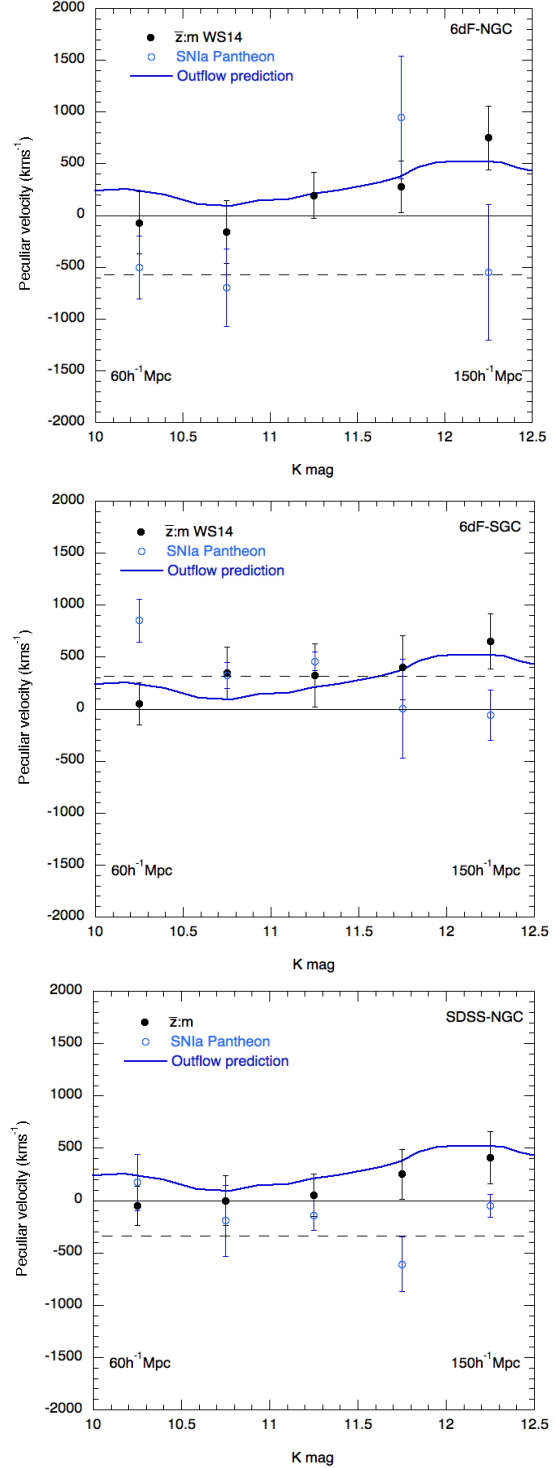


Figure 2. The WS14 peculiar velocities (filled circles) estimated from the residuals between the observed $\bar{z}(m)$ Hubble diagram and a homogeneous model in their three individual fields. The range $10.0 < K < 12.5$ translates to $60 \lesssim d \lesssim 150 h^{-1} \text{Mpc}$ via this model. WS14 found that bulk motion in the Local Group frame (solid horizontal line) was preferred by these data except in 6dF-SGC where galaxies appeared more at rest in the CMB frame (horizontal dashed line). Adding the Local Hole outflow model of Shanks et al (2019) in the Local Group frame (blue line) improves the fit in 6dF-SGC while maintaining it in 6dF-NGC and SDSS-NGC. The peculiar velocities from Pantheon SNIa (open circles) show less good agreement with the model at larger distances.

three areas, for completeness we first show in Fig. 1 the overall average density contrast $(\frac{dn}{n})_i$ found by combining the three areas of WS14 that leads to the $\frac{\Delta v}{v_H}(z)$ result shown in Fig. 1 of Shanks et al. (2019). Here, we find an overall median underdensity of $\approx -23\%$ out to $\approx 150h^{-1}\text{Mpc}$. Indeed, also from Fig. 1, the similarly combined SDSS-NGC + 6dF-NGC areas still show a $\approx -11\%$ median underdensity. Together, these results therefore support a roughly isotropic underdensity around our position as assumed in the above model, now shown as the solid blue lines in Figs. 2, 3.

3.2 Observed $\bar{z}(m)$ outflows and bulk motions

In Figs. 2 we summarise the WS14 peculiar velocity results in each of their three areas, as estimated via $\bar{z}(m)$. The closed circles show the residuals from the homogeneous $\bar{z}(m)$ model which represent the WS14 average peculiar velocity estimates in their three directions. The homogeneous $\bar{z}(m)$ model has also been used to relate the K magnitude of a $\bar{z}(m)$ bin to its luminosity distance, d . So the $K = 10.25 \pm 0.25$ bin corresponds to $d \approx 60h^{-1}\text{Mpc}$ and the $K = 12.25 \pm 0.25$ bin corresponds to $d \approx 150h^{-1}\text{Mpc}$, as indicated in Figs. 2, 3. WS14 corrected their galaxy redshifts into the Local Group frame (see WS14 eq. 10) which implies the Local Group is moving with 633 km s^{-1} with respect to the Cosmic Microwave Background.

Fig. 2 thus shows the $\bar{z}(m)$ peculiar velocities compared to the $v_{pec} = 0$ solid horizontal line that corresponds to galaxies lying at rest in the Local Group frame whereas the horizontal dashed line corresponds to the galaxies lying at rest in the CMB frame. Thus the former would indicate the Local Group and galaxies in that direction were participating in coherent bulk motion relative to the CMB. WS14 concluded that the results in the 6dF-NGC and SDSS-NGC directions were consistent with such a bulk motion while those in the 6dF-SGC direction were more consistent with the galaxies being at rest in the CMB frame. They noted that the 6dF-SGC result might still be consistent with bulk motion if there was an additional outflow component due to the enhanced underdensity in that direction.

In Figs. 2 we now compare the results for the above Local Hole outflow model of Shanks et al. (2019) to the $\bar{z}(m)$ peculiar velocity results of WS14. The model (solid blue line) as plotted in these Figures simply represents an adding of the outflow model to the $v_{pec} = 0$ (solid horizontal line) result expected if the galaxies are at rest in the Local Group frame. In the three areas this combined bulk flow plus outflow model looks consistent with these data. Thus the addition of the outflow model seems to have improved the bulk motion fit in the 6dF-SGC direction while not damaging the bulk motion fit too much in the other two directions.

Fig. 3 then shows the area weighted average of the observed peculiar velocities over all three directions. There is clearly now no sensitivity to bulk motion but these data can still be used to look for an outflow due to a global underdensity in this volume. We again see excellent agreement between the outflow model and the $\bar{z}(m)$ peculiar velocity estimates.

We have used χ^2 to compare the $\bar{z}(m)$ peculiar velocities with the predicted outflow model in each of the directions and then in the three directions combined (see Table

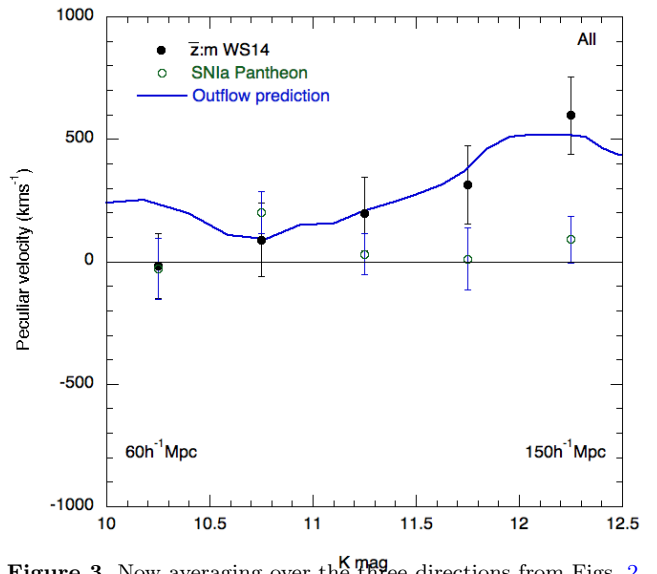


Figure 3. Now averaging over the three directions from Figs. 2, the overall peculiar velocities from $\bar{z}(m)$ (filled circles) show excellent agreement with the Local Hole outflow prediction of Shanks et al (2019) (blue line), here added to the model where all galaxies are assumed to be at rest in the Local Group frame (horizontal solid line). The peculiar velocities from Pantheon SNIa (open circles) show less good agreement at larger distances/magnitudes.

1). We have assumed the errors on the outflow model from Shanks et al. (2019). There are caveats on our application of these χ^2 tests which we discuss in Section 3.3 below. Nevertheless, we see that the χ^2 values for the $\bar{z}(m)$ velocities appear generally consistent with the model.

The observed WS14 peculiar velocities therefore seem to agree with the outflow model of Shanks et al. (2019) based on the WS14 Local Hole underdensity. Again it must be cautioned that much depends on the final $K = 12.5$, $r \approx 150h^{-1}\text{Mpc}$ v_{pec} point that WS14 regarded as uncertain, partly due to its amplitude. We also refer to WS14's caveat about the possible vulnerability of $\bar{z}(m)$ to evolution in the LF, although this is minimised by the low redshift range involved and our use of the K band. *Nevertheless, in this work we recognise for the first time the self-consistency of the WS14 Local Hole underdensity and peculiar velocity measurements, related through our dynamical outflow model.*

3.3 SNIa peculiar velocities compared to outflow model

We next compare the agreement between the peculiar velocities implied by SNIa and our outflow model. In Figs. 2, we see that the agreement between the SNIa Pantheon results and the outflow model data is poor in the fields with most SNIa i.e the 6dF-SGC and SDSS-NGC fields. In 6dF-NGC there is no inconsistency between these two but with only 6 SNIa the errors are large. Also note that there are zero SNIa in the $K = 11.25$ bin. Clearly, the agreement with the model appears poorer for the SNIa than the $\bar{z}(m)$ peculiar velocity estimates.

The all-sky results for 130 Pantheon SNIa in the usual magnitude range $10 < K < 12.5$ or $60 \lesssim d \lesssim 150h^{-1}\text{Mpc}$ are shown in Fig. 3 where they are seen to disagree with the Local Hole outflow prediction and the $\bar{z}(m)$ peculiar velocity

	$\bar{z}(m)$ χ^2 (d.f.)	$\bar{z}(m)$ p	SNIa χ^2 (d.f.)	SNIa p	No. SNIa
6dF-NGC	2.3778 (5)	0.79	0.6574 (4)	0.96	6
6dF-SGC	1.7763 (5)	0.88	18.114 (5)	2.8×10^{-3} (3.0σ)	29
SDSS-NGC	2.5244 (5)	0.77	26.491 (4)	2.5×10^{-5} (4.2σ)	20
All	2.4278 (5)	0.79	18.829 (5)	2.1×10^{-3} (3.1σ)	295

Table 1. χ^2 comparisons of the Local Hole outflow model of Shanks et al. (2019) with $\bar{z}(m)$ and SNIa peculiar velocity estimates. d.f. gives χ^2 degrees-of-freedom. p is the probability of a higher χ^2 value and σ is the equivalent 2-tailed Gaussian significance level.

estimates of WS14. This result at first looks similar to that of D’Arcy Kenworthy et al. (2019) who found no evidence of outflow in the Pantheon + Foundation + CSPDR3 datasets.

We again use χ^2 to compare the SNIa peculiar velocities with the predicted outflow model in each of the three WS14 directions and then in the three directions combined (see Table 1). We again assume the errors on the outflow model from Shanks et al. (2019). We see that the χ^2 values for the the SNIa peculiar velocities reject the model for the full sample and for the SDSS-NGC and 6dF-SGC sub-samples and are generally poorer fits to the model than the $\bar{z}(m)$ velocity estimates.

However, as previously noted, there are several issues which mean all the χ^2 results in Table 1 should only be treated as illustrative. First, we have ignored SNIa systematics which will contribute to the errors. Second, we have ignored covariances between the $\bar{z}(m)$ bins, the SNIa bins and the outflow model predictions. The results are also sensitive to how we have handled the errors on the model velocities in the χ^2 . All we claim is that since we have applied our assumptions consistently to both the $\bar{z}(m)$ and SNIa comparisons, so the *relative* goodness-of-fits given in Table 1 may be qualitatively believable and useful. With these caveats, we conclude that the outflow model appears in better agreement with the WS14 $\bar{z}(m)$ peculiar velocities than with the Pantheon SNIa data.

The lack of detection of outflow is confirmed by our analysis of the Pantheon SNIa survey over its full redshift range.¹ Here with 1048 SNIa we found a reduced $\chi^2 = 1.0558$ on 1046 degrees-of-freedom for the best fit $\Omega_m = 0.28 \pm 0.015$, $H_0 = 73.7 \pm 0.2 \text{ km s}^{-1} \text{ Mpc}^{-1}$ model with no outflow assumed. Assuming the isotropic outflow model predicted by our Local Hole results, we found a reduced $\chi^2 = 1.0593$ on 1046 degrees-of-freedom for the best fit $\Omega_m = 0.32 \pm 0.015$, $H_0 = 72.7 \pm 0.2 \text{ km s}^{-1} \text{ Mpc}^{-1}$ model. So the outflow model with slightly higher Ω_m and slightly lower H_0 fits the Hubble diagram less well but only by $\Delta\chi^2 = 3.66$ which, with only two parameters fitted, represents only a $\approx 1.4\sigma$ rejection of the outflow model.² This result broadly supports the reply of Shanks et al. (2019) to Riess et al. (2018a), that a small increase in Ω_m allows our Local Hole outflow model to be an acceptable fit to the SNIa Hubble diagram.

Finally, D’Arcy Kenworthy et al. (2019) claim that in

their bigger sample of 397 $0.023 < z < 0.15$ SNIa, our outflow prediction can be rejected in the all-sky case and in the particular WS14 directions. Shanks et al. (2019) assumed $z = 0.1$ as being typical of a SNIa sample used to estimate H_0 at $z < 0.15$, giving $v_{pec} = 540 \text{ km s}^{-1}$ from their Fig. 2 and $v_{pec}/cz = 1.8\%$. Now, this outflow prediction of $\Delta H_0 = H_0^{local}/H_0^{global} = 1.018$ translates to a change in their Hubble diagram intercepts of $\Delta a_B = a_B - a_B^{FLRW} = \log_{10}(\Delta H_0) = 0.0077$. Based on the all-sky fits in their Table 1 (and Fig. 3a), $\Delta a_B = 0.0077$ is only rejected at $1.9 - 2.2\sigma$ in the $0.023 < z < 0.15$ and $0.01 < z < 0.5$ ranges. Similarly, in their Table 1 (and Fig. 5b), $\Delta a_B^{z < 0.05} = 0.0077$ is only rejected at 0.8σ in the $0.01 < z < 0.5$ range in the WS14 fields. D’Arcy Kenworthy et al. (2019) here quote a 2.6σ rejection taking $v_{pec} = 520 \text{ km s}^{-1}$ at $z = 0.05$ from Fig. 2 of Shanks et al. (2019). But volume weighting the outflow model gives 365 km s^{-1} at $z \approx 0.04$ leading to a 2.0σ rejection. So the rejection of the outflow model of Shanks et al. (2019) is only at the $\approx 1 - 2\sigma$ level and thus perhaps less strong in the larger local SNIa samples of D’Arcy Kenworthy et al. (2019) than in the Pantheon sub-sample.

4 CONCLUSIONS

WS14 presented strong evidence from both galaxy counts and galaxy number redshift distributions for a local inhomogeneous underdensity out to $\approx 150 \text{ h}^{-1} \text{ Mpc}$. This ‘Local Hole’ underdensity was somewhat more pronounced in the 6dF-SGC (SGP) direction but we have first shown here that the underdensity persists after averaging over all three directions (see Fig. 1). In the Southern sky, the underdensity shown by the galaxy redshift distribution is further strongly supported by the redshift distribution of REFLEX II X-ray galaxy clusters (see Fig. 8 of Böhringer et al. 2015). Böhringer et al. (2019) have recently also similarly found that their new Northern cluster samples are in good agreement with the WS14 $n(z)$ results. Combined, their CLAS-SIX cluster survey covers 66% of the sky. Thus despite the criticism by D’Arcy Kenworthy et al. (2019) of WS14 areas only covering $\approx 22\%$ of the sky, this agreement with, and extra coverage of, the X-ray cluster survey supports the possibility that the Local Hole may feature over most of the local volume out to $\approx 150 \text{ h}^{-1} \text{ Mpc}$. This further motivates the assumption of approximate isotropy made in the dynamical outflow model of Shanks et al. (2019) (see also Hoscheit & Barger (2018)).

We note that Jasche & Lavaux (2019) failed to detect a Local Hole underdensity in 2M++ data. Nevertheless their Figs. 10(a, b, c) show some similarity to our Fig. 1 and Figs. 3(a, b) of WS14 but perhaps with different normalisations. Although sophisticated in their treatment of peculiar veloc-

¹ The caveat made above about ignoring the systematic errors in the SNIa peculiar velocity estimates also applies here.

² Note that here we have fitted in the Local Group frame whereas Shanks et al. (2019) fitted in the CMB frame after correcting for peculiar motions estimated from 2M++ (Carrick et al. 2015) and found that the outflow model gave a marginally better fit than no outflow.

ities, in deriving density-redshift relations [Jasche & Lavaux \(2019\)](#) assume an LF independent of galaxy colour and morphology unlike [WS14](#) and with no attempt to solve for the LF independently like [Whitbourn & Shanks \(2016\)](#). It would also be interesting to check that their assumed LF and normalisation used to estimate their density-redshift relations are consistent with fainter *K*-band galaxy counts (c.f. Figs. 5, 6 of [WS14](#)).

Overall, in Fig. 3 the outflow model of [Shanks et al. \(2019\)](#) also seems to fit the $\bar{z}(m)$ data well. However, there is a discrepancy with the SNIa data from the Pantheon sample which would prefer zero outflow as the best fit. But we have argued that the larger Pantheon+Foundation+CSPDR3 SNIa sample of [D’Arcy Kenworthy et al. \(2019\)](#) only excludes the void at the $1 - 2\sigma$ level. Of course, there are still possible issues with the $\bar{z}(m)$ results: they need substantial correction for the same local inhomogeneities that are the subject of the $n(m)$ and $n(z)$ studies; they assume that there are no evolutionary or environmental effects on the *K*-band LF used as a standard candle. The highest redshift $\bar{z}(m)$ is also most sensitive to systematic effects. *But the agreement between the observed $\bar{z}(m)$ and the v_{pec} outflow model is impressive, adding to the strong evidence for the Local Hole from the basic count and redshift survey data of WS14.*

In terms of anisotropic flows, [WS14](#) originally found that in two directions the $\bar{z}(m)$ peculiar velocities implied the galaxies were exhibiting bulk motions out to $\approx 150h^{-1}\text{Mpc}$ in the sense that the galaxies appeared to be moving coherently with the Local Group. In the other 6dF-SGC direction, that showed the biggest underdensity, the result was more consistent with galaxies being at rest in the CMB frame with no bulk motion. The suggestion by [WS14](#) that the addition of an outflow component might improve the agreement with the bulk flows found in the other two directions now seems to be supported by the current outflow model. While improving the fit of the $\bar{z}(m)$ peculiar velocities to the bulk motion solution in the 6dF-SGC direction the model maintains the bulk flow solution in the other two directions.

We conclude that an outflow component due to the Local Hole coupled with a bulk motion within an $\approx 150h^{-1}\text{Mpc}$ radius in the direction of motion of the Local Group towards the Shapley supercluster give a self-consistent description of the [WS14](#) density and velocity fields implied by $n(z)$ and $\bar{z}(m)$ statistics. The size of the resulting reduction in H_0 is at the $\approx 2 - 3\%$ level needed to reconcile the reduced ‘tension’ between the value of $H_0 = 67.4 \pm 1.7 \text{ km s}^{-1} \text{ Mpc}^{-1}$ of [Planck Collaboration et al. \(2018\)](#) and at least the $H_0 = 69.8 \pm 1.9 \text{ km s}^{-1} \text{ Mpc}^{-1}$ estimated from the TRGB distance scale of [Freedman et al. \(2019\)](#). The reasons for the discrepancy with the Pantheon SNIa results are unclear but we have argued there is less disagreement with the bigger Pantheon+Foundation+CSPDR3 SNIa survey as used by [D’Arcy Kenworthy et al. \(2019\)](#). It will be interesting to see how the SNIa results improve at least in the Southern Hemisphere when more isotropic and better sampled SNIa searches start with LSST in the next few years.

ACKNOWLEDGEMENTS

We thank D. Scolnic (Duke University, USA) for supplying full information for the Pantheon SNIa sample. We thank H.

Böhringer (MPE, Germany) for informing us of the Northern Hemisphere CLASSIX X-ray cluster results prior to publication. Valuable comments from an anonymous referee also significantly improved the quality and clarity of the paper.

REFERENCES

- Böhringer H., Chon G., Bristow M., Collins C. A., 2015, *A&A*, **574**, A26
- Böhringer H., Chon G., Collins C. A., 2019, arXiv e-prints, p. arXiv:1907.12402
- Busswell G. S., Shanks T., Frith W. J., Outram P. J., Metcalfe N., Fong R., 2004, *MNRAS*, **354**, 991
- Carrick J., Turnbull S. J., Lavaux G., Hudson M. J., 2015, *MNRAS*, **450**, 317
- D’Arcy Kenworthy W., Scolnic D., Riess A., 2019, arXiv e-prints, Davis T. M., Scrimgeour M. I., 2014, *MNRAS*, **442**, 1117
- Davis M., Nusser A., Masters K. L., Springob C., Huchra J. P., Lemson G., 2011, *MNRAS*, **413**, 2906
- Dekel A., Eldar A., Kolatt T., Yahil A., Willick J. A., Faber S. M., Courteau S., Burstein D., 1999, *ApJ*, **522**, 1
- Feix M., Branchini E., Nusser A., 2017, *MNRAS*, **468**, 1420
- Freedman W. L., et al., 2019, *ApJ*, **882**, 34
- Frith W. J., Busswell G. S., Fong R., Metcalfe N., Shanks T., 2003, *MNRAS*, **345**, 1049
- Hoscheit B. L., Barger A. J., 2018, *ApJ*, **854**, 46
- Jasche J., Lavaux G., 2019, *A&A*, **625**, A64
- Keenan R. C., Barger A. J., Cowie L. L., Wang W.-H., Wold I., Trouille L., 2012, *ApJ*, **754**, 131
- Lauer T. R., Postman M., 1992, *ApJ*, **400**, L47
- Lauer T. R., Postman M., 1994, *ApJ*, **425**, 418
- Lukić V. V., Haridasu B. S., Vittorio N., 2019, arXiv e-prints, p. arXiv:1907.11219
- Lynden-Bell D., Faber S. M., Burstein D., Davies R. L., Dressler A., Terlevich R. J., Wegner G., 1988, *ApJ*, **326**, 19
- Macaulay E., Feldman H., Ferreira P. G., Hudson M. J., Watkins R., 2011, *MNRAS*, **414**, 621
- Macaulay E., Feldman H. A., Ferreira P. G., Jaffe A. H., Agarwal S., Hudson M. J., Watkins R., 2012, *MNRAS*, **425**, 1709
- Mathewson D. S., Ford V. L., Buchhorn M., 1992, *ApJ*, **389**, L5
- Nusser A., 2014, *ApJ*, **795**, 3
- Nusser A., 2016, *MNRAS*, **455**, 178
- Nusser A., Branchini E., Davis M., 2011, *ApJ*, **735**, 77
- Odderskov I., Hannestad S., Brandbyge J., 2017, *J. Cosmology Astropart. Phys.*, **2017**, 022
- Planck Collaboration et al., 2018, preprint, (arXiv:1807.06209)
- Pustilnik S. A., Tepliakova A. L., Makarov D. I., 2019, *MNRAS*, **482**, 4329
- Redlich M., Bolejko K., Meyer S., Lewis G. F., Bartelmann M., 2014, *A&A*, **570**, A63
- Riess A. G., Casertano S., Kenworthy D., Scolnic D., Macri L., 2018a, arXiv e-prints, p. arXiv:1810.03526
- Riess A. G., et al., 2018b, *ApJ*, **855**, 136
- Riess A. G., et al., 2018c, *ApJ*, **861**, 126
- Rizzi L., Tully R. B., Shaya E. J., Kourkchi E., Karachentsev I. D., 2017, *ApJ*, **835**, 78
- Scolnic D. M., et al., 2018, *ApJ*, **859**, 101
- Scrimgeour M. I., et al., 2016, *MNRAS*, **455**, 386
- Shanks T., Stevenson P. R. F., Fong R., MacGillivray H. T., 1984, *MNRAS*, **206**, 767
- Shanks T., Hogarth L., Metcalfe N., 2018, arXiv e-prints, p. arXiv:1810.07628
- Shanks T., Hogarth L. M., Metcalfe N., 2019, *MNRAS*, **484**, L64
- Soneira R. M., 1979, *ApJ*, **230**, L63
- Spergel D. N., et al., 2003, *ApJS*, **148**, 175
- Tonry J. L., Blakeslee J. P., Ajhar E. A., Dressler A., 2000, *ApJ*, **530**, 625

- Tully R. B., Shaya E. J., Karachentsev I. D., Courtois H. M., Kocevski D. D., Rizzi L., Peel A., 2008, [ApJ](#), **676**, 184
- Tully R. B., Courtois H. M., Sorce J. G., 2016, [AJ](#), **152**, 50
- Turnbull S. J., Hudson M. J., Feldman H. A., Hicken M., Kirshner R. P., Watkins R., 2012, [MNRAS](#), **420**, 447
- Watkins R., Feldman H. A., 2015, [MNRAS](#), **447**, 132
- Watkins R., Feldman H. A., Hudson M. J., 2009, [MNRAS](#), **392**, 743
- Whitbourn J. R., Shanks T., 2014, [MNRAS](#), **437**, 2146
- Whitbourn J. R., Shanks T., 2016, [MNRAS](#), **459**, 496
- Wojtak R., Knebe A., Watson W. A., Iliev I. T., Heß S., Rapetti D., Yepes G., Gottlöber S., 2014, [MNRAS](#), **438**, 1805
- Wu H.-Y., Huterer D., 2017, [MNRAS](#), **471**, 4946